Static capacitance at the electrochemical liquid-liquid interface between ionic liquids and eutectic Ga-In alloy measured using the pendant drop method

Naoya NISHI*, Yasuro KOJIMA, Seiji KATAKURA, and Tetsuo SAKKA

Department of Energy and Hydrocarbon Chemistry, Graduate School of Engineering, Kyoto University, Kyoto 615-8510, Japan

*Correspondence should be addressed

Tel: +81-75-383-2491

Email: nishi.naoya.7e@kyoto-u.ac.jp

Abstract

Static differential capacitance (C_{dc}) at the liquid-liquid interface between ionic liquids (ILs) and eutectic Ga-In alloy (EGaIn) has been measured using the pendant drop method for two ILs: 1-ethyl-3-methylimidazolium tetrafluoroborate ($[C_2mim^+]BF_4^-$) and 1-octyl-3-methylimidazolium bis(nonafluorobutanesulfonyl)amide ($[C_8mim^+][C_4C_4N^-]$). The potentials of zero charge for the IL|EGaIn interfaces are shifted compared with the IL|Hg interfaces with an amount that can be considered by the difference in the work functions of EGaIn and Hg. The measured C_{dc} at the $[C_2mim^+]BF_4^-$|EGaIn interface has well reproduced the camel-shape potential dependence of C_{dc} at the Hg interface of the same IL at the negatively charged potential region. This suggests that there are few specific interaction between the IL ions with EGaIn and Hg. The $[C_8mim^+][C_4C_4N^-]$|EGaIn has been compared with the $[C_8mim^+]BF_4^-$|Hg interface where IL-cation is the same but IL-anion is different. Also in that case C_{dc} is similar to each other at the negatively charged potential region, which means that accumulated C_8mim^+ ions at the interface mainly govern the C_{dc} behavior.

Keywords: electric double layer; interfacial tension; electrocapillary curve; potential of zero charge

1 Introduction

Ionic liquids (ILs), which are liquid salts composed of cations and anions, have been extensively studied for the possible electrochemical applications.[1–4] Because of the nature of ILs that contain no neutral solvent molecules, the conventional models[5–7] for the electrical double layer (EDL) and the differential capacitance, C, of electrolyte solutions are not applicable to ILs. Alternative models have been proposed for the EDL behavior in ILs.[3,8–10] The models suggest that the dependence of C on the potential, E, for the EDL of ILs shows one-hump or two-hump camel shape around the potential of zero charge, E_{pzc}, depending on the size of charged and neutral moieties of IL ions. The camel shape is significantly different from U shape in the conventional models, reflecting the peculiarity of the EDL of ILs. In contrast to the progress of the understanding of the EDL of ILs from the theoretical side, experimental confirmation of the predicted IL-peculiar behavior is not straightforward. It has been found, from studies using electrochemical impedance spectroscopy (EIS), that C for the EDL of ILs has strong frequency dependence[11–18] and shows potential hysteresis,[11,19–21] both of which seem to result from the structural ordering of IL interface[22–29] and the ultraslow dynamics[29–38] of such ordered structure. These tendencies have hampered rigorous evaluation of C experimentally. One way to avoid such troubles is to evaluate static differential capacitance, C_{dc}, in other words, C at equilibrium. Because theoretically predicted differential capacitance is also static, experimental evaluation of C_{dc} is invaluable so that we can compare experimental and theoretical behaviors, and obtain feedbacks for the improvement of the theories.

Recently, we experimentally obtained C_{dc} from the thermodynamic analysis of the electrocapillarity (interfacial tension, γ, as a function of E) at the IL|Hg interface using the pendant drop method.[39,40] The pendant drop method is a static method unlike other methods such as EIS,[41–50] drop time method,[42,44,51–54] and drop weight method[55] utilized to study the EDL of ILs, and therefore, the measurements are not affected by the ultraslow dynamics described above. C_{dc} by the pendant drop method enabled us to reproduce the one-hump[39,40] and two-hump[39] camel-shape behavior predicted by the theories (see open symbols around E_{pzc}, vertical dotted lines, in Figs.2a and 2b, respectively). In addition to the predicted one, two unexpected behaviors of C_{dc} was also found. One is steep rise in C_{dc} at potentials far from E_{pzc} (see open symbols in Fig.2). This phenomenon was also observed for the electrochemical interface between Hg and an aqueous solution (W)[56,57] and is probably caused by densification of ions[58] in the EDL for the IL case. The other phenomenon was at potentials with moderate $|E - E_{\mathrm{pzc}}|$ where C_{dc} deviates downward from the fitted curve from the theories and shows a dip (see the downward deviation of open symbols from dashed lines in Fig.2). The latter seems peculiar to ILs and is likely to result from the rigid structure of the ionic multilayers that are stabilized to have alternating nature when the interface is charged up. The latter phenomenon might be characteristic to Hg electrode due to possible specific interaction between IL-ions and Hg. To verify the generality of the phenomenon, it is desirable to study C_{dc} for the EDL of ILs with other liquid electrodes.

In the present study, we adopted eutectic Ga-In (EGaIn), a liquid alloy, for the liquid electrode. Funda-

mental electrochemical properties of the W|EGaIn interface has been studied for decades.[59–65] The adsorption behavior of surface-active molecules and ions in W was compared at the interfaces of EGaIn and Hg, revealing that these two liquid electrodes show basically similar adsorption behavior with some difference.[64,65] With regard to the electrochemistry of ILs, electrodeposition of Ga[66–70] and In[71–75] in ILs has been intensively studied. We will show in the present study that the C_{dc} behavior at the IL|EGaIn interface measured using the pendant drop method reproduces that at the IL|Hg interface, supporting that the phenomena observed at the IL|Hg interface are universal for the EDL in ILs.

2 Experimental

$[C_2mim^+]BF_4^-$ ($C_n mim^+$: 1-alkyl-3-methylimidazolium) was purchased from Kanto Chemical and was used without further purification. $[C_8mim^+][C_4C_4N^-]$ ($C_4C_4N^-$: bis(nonafluorobutanesulfonyl)amide) was prepared from synthesized[39] $[C_8mim^+]Cl^-$ and purchased $Li^+[C_4C_4N^-]$ (Mitsubishi Material), and then was purified.[30,76] Before measurements, volatile impurities were removed from the ILs by using a rotary oil pump for more than 3 h at 60 °C. EGaIn (99.99%, Alfa Aesar) was stored in an 1M HCl aqueous solution. EGaIn was washed with methanol and water to remove HCl and then dried in an Ar atmosphere just before use.

The details of the pendant drop method have been reported previously.[39,40] Briefly, a pendant drop of EGaIn hanging from a glass tube immersed in IL was imaged and the outline of the drop was numerically fitted with the theoretical curve. In the fitting, the densities, ρ, of IL and EGaIn were fixed and the interfacial tension, γ, was evaluated as a variable parameter. The ρ values for $[C_2mim^+]BF_4^-$ and $[C_8mim^+][C_4C_4N^-]$ were measured to be 1.279 and 1.505 g cm^{-3}, respectively, at 25.0 °C by using a density meter (DA-505, KEM). For the ρ value for EGaIn, 6.25 g cm^{-3} was taken from literature.[77] An Ag wire coated with AgCl was directly immersed in the IL as a quasi-reference electrode (QRE), and a Pt coiled wire as a counter electrode (CE). The potential of the EGaIn working electrode (WE) with respect to the Ag/AgCl QRE, denoted as E, was controlled using a PC-controlled potentiostat (HA1010mM1A, Hokuto Denko). At each potential, measurements were continued for sufficiently long time, typically more than 5 min to equilibrate the interfacial structure at the IL|Hg interface. The γ value that became independent of time was adopted as γ in equilibrium at the potential. Measurements were performed at 25.0±0.1 °C. During the measurements, Ar gas was kept flowing on the IL surface in the cell. To obtain the surface charge density on electrode, q ($= -\partial\gamma/\partial E$), the electrocapillarity data was numerically differentiated. Quadratic least squares regression with weight from experimental error was applied for each nine consecutive data points of γ and the slope of the regression curve at the potential of the center data point was evaluated. C_{dc} ($= \partial q/\partial E$) was similarly obtained from the E dependence of q.

3 Results and Discussion

Figures 1a and 1b show linear sweep voltammograms at the $[C_2mim^+]BF_4^-$|EGaIn interface and the $[C_8mim^+][C_4C_4N^-]$|EGaIn interface, respectively. Both the interfaces show the potential window with a width of around 2 V. During the positive-going scan, we observed small anodic current peaks at −1.75 (Fig.1a) and −1.96 V (Fig.1b) and found that film is formed at the interfaces at potentials more positive than the peak potential. The composition of the film is unclear, however, we consider that it is either Ga_2O_3[78] or salts of Ga ion with the IL anions, insoluble to the ILs. The effect of the film formation on C_{dc} will be discussed in Appendix. The discussion suggested that the measured C_{dc} is still valid for the evaluation of the EDL of the ILs semi-quantitatively.

The electrocapillary curves at the $[C_2mim^+]BF_4^-$|EGaIn interface (red square) and the $[C_8mim^+][C_4C_4N^-]$|EGaIn interface (blue diamond) are shown in Fig.1c. Also shown is the electrocapillary curve at the $[C_2mim^+]BF_4^-$|Hg interface (black open circle) from our previous study[39] for comparison. The curves for the two EGaIn interfaces exhibited parabolic shape which is typical for electrocapillary curves as shown at the $[C_2mim^+]BF_4^-$|Hg interface (black open circle). Only negative branch of parabola was measured and the data at more positive potentials was inaccessible due to the film formation. In spite of no distinctly observable apex of the parabola, E_{pzc} was roughly estimated to be around −0.8 V for the two EGaIn interfaces by the extrapolation of the q vs. E plots to the $q = 0$ intercept.[39,40] The E_{pzc} at the $[C_2mim^+]BF_4^-$|EGaIn interface is −0.4 V shifted from that at the corresponding Hg interface (−0.42 V).[39] This shift is mainly caused by the difference of the work functions between EGaIn (4.1-4.2 eV[79]) and Hg (4.49 eV[80]), because it is known that E_{pzc} for the interface between metal and an aqueous solution has linear relationship with a slope of unity with the work function of metal.[81] The γ value at E_{pzc} for the EGaIn interface are 0.11 N m^{-1} higher than that for the Hg interface, when compared for the same IL, $[C_2mim^+]BF_4^-$ (red square and black open circle). This γ difference agrees with that between the surface tension of EGaIn (0.595 N m^{-1} at 32 °C[62]) and Hg (0.485 N m^{-1} at 25 °C[82]), implying that little specific interaction between IL ions with both EGaIn and Hg, as is the case for the W interfaces of EGaIn and Hg.[59,62]

By numerically differentiating γ with respect to E twice, C_{dc} was evaluated. Figures 2a and 2b show C_{dc} as a function of E at the $[C_2mim^+]BF_4^-$|EGaIn interface (red square) and the $[C_8mim^+][C_4C_4N^-]$|EGaIn interface (blue diamond), respectively. Both show dips in C_{dc} at −1.3 V. These dips reproduce previous results for the Hg interface of ILs,[39] which are also shown in Fig.2. In Fig.2a, one can compare the C_{dc} for the EGaIn (red square) and Hg (black open circle) interface of $[C_2mim^+]BF_4^-$ and may notice that the EGaIn data significantly resembles to the Hg one with a shift of −0.65 V. Again, the negative shift is mainly ascribable to the difference in the work functions for EGaIn and Hg. The amount of the shift is somewhat greater than that roughly estimated from Fig.1c. The dip cannot be explained by the theories for the EDL of ILs as described in Introduction. While the steep rise in C_{dc} at $E \ll E_{pzc}$ was clearly observed for the $[C_2mim^+]BF_4^-$|Hg interface (black open circle), it is not discernible for the EGaIn interface (red square) within the measured potential

range. This is probably also due to the potential shift and the C_{dc} would rise at more negative potentials.

In Fig.2b the $[C_8mim^+][C_4C_4N^-]$|EGaIn interface (blue diamond) is compared with the Hg interface of $[C_8mim^+]BF_4^-$[39] (black open square), an IL having the same cation (but different anion). Because cations are accumulated and anions are depleted in the EDL at $E < E_{pzc}$, the behavior of C_{dc} at $E < E_{pzc}$ is likely to be affected more by the IL cation rather than the IL anion. Like the Fig.2a case, these C_{dc} data in Fig.2b resemble each other with a −0.55 V shift for the EGaIn data. The similarity of the C_{dc} data at $E < E_{pzc}$ for the ILs having the same cation suggests that C_{dc} is mainly determined by the IL cation at $E < E_{pzc}$. On the other hand, the C_{dc} behavior at $E > E_{pzc}$ for the Hg interface of $[C_2mim^+]BF_4^-$ (black open circle in Fig.2a) and $[C_8mim^+]BF_4^-$ (black open square in Fig.2b) is different, although both still exhibit dips in C_{dc}. BF_4^- ions, accumulated at $E > E_{pzc}$, are smaller than the imidazolium cations, C_2mim^+ and C_8mim^+. In order to occupy the EDL and to govern the C_{dc} behavior, smaller ions need greater $|q|$,[83] and also greater $|E - E_{pzc}|$ unless the existence of small ions leads to extraordinarily high C_{dc}. Therefore the smaller BF_4^- anions are likely to need greater $|E-E_{pzc}|$ than the imidazolium cations. The amplitude of the dips is deeper and broader for the $[C_8mim^+][C_4C_4N^-]$|EGaIn interface (blue diamond in Fig.2b) than the corresponding interface of $[C_2mim^+]BF_4^-$ (red square in Fig.2a). This can be explained with the difference in the rigidness and stability of the EDL structure: C_8mim^+ ions form rigid and stable ionic multilayers in the EDL with their octyl chain aligned perpendicular to the interface.[44]

In summary, the C_{dc} at the EGaIn alloy interface of ILs was evaluated by using the pendant drop method. At potentials for the negatively charged interface, C_{dc} well reproduced previous data at the IL|Hg interface, suggesting that specific interaction of IL ions with EGaIn and Hg are negligible and that the EDL structure of ILs becomes rigid and decreases C_{dc} at moderately charged interface of ILs.

Acknowledgements

This work was partly supported by a JSPS KAKENHI (Nos. 26410149, 26248004, 16H04216).

Appendix

In the LSVs at the EGaIn interface of ILs, we observed positive current peaks due to film formation at the interface. The contribution of the film to the C_{dc} measured using the pendant drop method was subtracted by using the following procedure. The modified C_{dc} ($C_{dc,EDL}$ described below) are semi-quantitatively similar to the measured C_{dc} suggesting that the discussion in Results and Discussion, which was made based on the measured C_{dc}, remains valid.

EIS can give us the differential capacitance under ac potential perturbation, C_{ac}. In the present case, C_{ac} can be modeled as a series connection of the EDL component of IL, $C_{ac,EDL}$, and that of the film, $C_{ac,film}$.

Therefore, C_{ac} may be represented with the reciprocal sum of them as,

$$\frac{1}{C_{ac}} = \frac{1}{C_{ac,film}} + \frac{1}{C_{ac,EDL}} \tag{A1}$$

Because the plots of $C_{ac,EDL}$ with respect to E exhibit featureless behavior,[40] $C_{ac,EDL}$ is assumed to be independent of E. On the other hand, it is known that $C_{ac,EDL}$ has strong frequency dependence as presented in Introduction, and that is why it is valuable to evaluate C_{dc} by the pendant drop method. For the film, such behavior with respect to E and frequency can be regarded totally opposite; strong E dependence and no frequency dependence. The former is based on the observation during the LSVs where film is formed only at potentials more positive than the peak potential. For the latter general capacitive behavior is assumed. Since the film is not formed at potentials more negative than the peak potential in the LSVs, we can evaluate the E independent $C_{ac,EDL}$ from the averaged C_{ac} values at such potentials: $-2.1 \sim -1.8$ V for the $[C_2mim^+]BF_4^-$|EGaIn interface and $-2.2 \sim -1.95$ V for the $[C_8mim^+][C_4C_4N^-]$|EGaIn interface (see Fig.A1). From the $C_{ac,EDL}$ values, we evaluate the E dependent $C_{ac,film}$ by using Eq. A1.

For C_{dc}, the reciprocal sum may be written similarly to the ac potential perturbation case,

$$\frac{1}{C_{dc}} = \frac{1}{C_{dc,film}} + \frac{1}{C_{dc,EDL}} \tag{A2}$$

By using the Eq. A2 combined with the measured C_{dc} and the evaluated $C_{dc,film}$ ($= C_{ac,film}$), $C_{dc,EDL}$ can be estimated.

EIS was performed to evaluate C_{ac} with the electrochemical cell same as that for the pendant drop method. To prevent the change in the interfacial area caused by the potential perturbation, the interface was formed not as a drop shape but as a disk shape at the tip of the glass tube with an inner diameter of 2.0 mm. A PC-controlled potentiostat (CompactStat, Ivium Technologies) was used with an ac potential amplitude of 10 mV and a frequency of 500 and 100 Hz for $[C_2mim^+]BF_4^-$ and $[C_8mim^+][C_4C_4N^-]$, respectively.

C_{ac} was evaluated from the measured impedance, Z, by assuming a simple capacitor behavior as

$$C_{ac} = -\frac{1}{\omega \mathrm{Im}[Z] A} \tag{A3}$$

where ω is angular frequency and A is the interfacial area (3.1 mm^2).

Figure A1 shows the estimated $C_{dc,EDL}$ as a function of E along with C_{ac} measured using ac voltammetry and C_{dc} measured using the pendant drop method. The latter is the same as C_{dc} in Figs.2a and 2b. The difference between $C_{dc,EDL}$ and C_{dc} is not significant, demonstrating that the discussion of the EDL of ILs using C_{dc} in Results and Discussion is valid semi-quantitatively.

References

(1) M. Armand, F. Endres, D. R. Macfarlane, H. Ohno, and B. Scrosati, *Nat. Mater.*, 2009, **8**, 621–629.

(2) H. Ohno, ed. , *Electrochemical Aspects of Ionic Liquids*, Wiley, Hoboken, 2nd ed., 2011.

(3) M. V. Fedorov and A. A. Kornyshev, *Chem. Rev.*, 2014, **114**, 2978–3036.

(4) R. Hayes, G. G. Warr, and R. Atkin, *Chem. Rev.*, 2015, **115**, 6357–6426.

(5) L. G. Gouy, *J. Phys.*, 1910, **9**, 457–468.

(6) D. L. Chapman, *Phil. Mag.*, 1913, **25**, 475–481.

(7) O. Stern, *Z. Elektrochem.*, 1924, **30**, 508–516.

(8) A. A. Kornyshev, *J. Phys. Chem. B*, 2007, **111**, 5545–5557.

(9) M. S. Kilic, M. Z. Bazant, and A. Ajdari, *Phys. Rev. E*, 2007, **75**, 021502(1–16).

(10) K. B. Oldham, *J. Electroanal. Chem.*, 2008, **613**, 131–138.

(11) V. Lockett, R. Sedev, J. Ralston, M. Horne, and T. Rodopoulos, *J. Phys. Chem. C*, 2008, **112**, 7486–7495.

(12) M. Gnahm, T. Pajkossy, and D. M. Kolb, *Electrochim. Acta*, 2010, **55**, 6212–6217.

(13) M. Drüschler, B. Huber, and B. Roling, *J. Phys. Chem. C*, 2011, **115**, 6802–6808.

(14) T. Pajkossy and D. M. Kolb, *Electrochem. Commun.*, 2011, **13**, 284–286.

(15) B. Roling, M. Drüschler, and B. Huber, *Faraday Discuss.*, 2012, **154**, 303–311.

(16) Y. Su, J. Yan, M. Li, M. Zhang, and B. Mao, *J. Phys. Chem. C*, 2013, **117**, 205–212.

(17) L. Siinor, R. Arendi, K. Lust, and E. Lust, *J. Electroanal. Chem.*, 2013, **689**, 51–56.

(18) J. Wallauer, M. Drüschler, B. Huber, and B. Roling, *Z. Naturforsch. B*, 2013, **68**, 1143–1153.

(19) T. R. Gore, T. Bond, W. Zhang, R. W. J. Scott, and I. J. Burgess, *Electrochem. Commun.*, 2010, **12**, 1340–1343.

(20) M. Drüschler, B. Huber, S. Passerini, and B. Roling, *J. Phys. Chem. C*, 2010, **114**, 3614–3617.

(21) M. T. Alam, J. Masud, M. M. Islam, T. Okajima, and T. Ohsaka, *J. Phys. Chem. C*, 2011, **115**, 19797–19804.

(22) M. Mezger, H. Schröder, H. Reichert, S. Schramm, J. S. Okasinski, S. Schöder, V. Honkimäki, M. Deutsch, B. M. Ocko, J. Ralston, M. Rohwerder, M. Stratmann, and H. Dosch, *Science*, 2008, **322**, 424–428.

(23) R. Atkin, S. Z. El Abedin, R. Hayes, L. H. S. Gasparotto, N. Borisenko, and F. Endres, *J. Phys. Chem. C*, 2009, **113**, 13266–13272.

(24) N. Nishi, Y. Yasui, T. Uruga, H. Tanida, T. Yamada, S. Nakayama, H. Matsuoka, and T. Kakiuchi, *J. Chem. Phys.*, 2010, **132**, 164705(1–6).

(25) N. Nishi, T. Uruga, H. Tanida, and T. Kakiuchi, *Langmuir*, 2011, **27**, 7531–7536.

(26) N. Nishi, K. Kasuya, and T. Kakiuchi, *J. Phys. Chem. C*, 2012, **116**, 5097–5102.

(27) J. M. Black, M. B. Okatan, G. Feng, P. T. Cummings, S. V. Kalinin, and N. Balke, *Nano Energy*, 2015, **15**, 737–745.

(28) N. Nishi, T. Uruga, and H. Tanida, *J. Electroanal. Chem.*, 2015, **759**, 129–136.

(29) P. Reichert, K. S. Kjar, T. B. van Driel, J. Mars, J. W. Ochsmann, D. Pontoni, M. Deutsch, M. M. Nielsen, and M. Mezger, *Faraday Discuss.*, 2017, , in press.

(30) Y. Yasui, Y. Kitazumi, R. Ishimatsu, N. Nishi, and T. Kakiuchi, *J. Phys. Chem. B*, 2009, **113**, 3273–3276.

(31) I. Bou-Malham and L. Bureau, *Soft Matter*, 2010, **6**, 4062–4065.

(32) S. Makino, Y. Kitazumi, N. Nishi, and T. Kakiuchi, *Electrochem. Commun.*, 2011, **13**, 1365–1368.

(33) M. Drüschler, N. Borisenko, J. Wallauer, C. Winter, B. Huber, F. Endres, and B. Roling, *Phys. Chem. Chem. Phys.*, 2012, **14**, 5090–5099.

(34) N. Nishi, Y. Hirano, T. Motokawa, and T. Kakiuchi, *Phys. Chem. Chem. Phys.*, 2013, **15**, 11615–11619.

(35) M. B. Singh and R. Kant, *J. Phys. Chem. C*, 2014, **118**, 8766–8774.

(36) A. Uysal, H. Zhou, G. Feng, S. S. Lee, S. Li, P. T. Cummings, P. F. Fulvio, S. Dai, J. K. McDonough, Y. Gogotsi, and P. Fenter, *J. Phys.-Condes. Matter*, 2015, **27**, 032101(1–9).

(37) T. Jänsch, J. Wallauer, and B. Roling, *J. Phys. Chem. C*, 2015, **119**, 4620–4626.

(38) C. Müller, K. Németh, S. Vesztergom, T. Pajkossy, and T. Jacob, *Phys. Chem. Chem. Phys.*, 2016, **18**, 916–925.

(39) N. Nishi, A. Hashimoto, E. Minami, and T. Sakka, *Phys. Chem. Chem. Phys.*, 2015, **17**, 5219–5226.

(40) N. Nishi, S. Yasui, A. Hashimoto, and T. Sakka, *J. Electroanal. Chem.*, 2017, **789**, 108–113.

(41) R. J. Gale and R. A. Osteryoung, *Electrochim. Acta*, 1980, **25**, 1527–1529.

(42) C. Nanjundiah, S. F. McDevitt, and V. R. Koch, *J. Electrochem. Soc.*, 1997, **144**, 3392–3397.

(43) Y. Z. Su, Y. C. Fu, J. W. Yan, Z. B. Chen, and B. W. Mao, *Angew. Chem.-Int. Edit.*, 2009, **48**, 5148–5151.

(44) M. T. Alam, M. M. Islam, T. Okajima, and T. Ohsaka, *J. Phys. Chem. C*, 2009, **113**, 6596–6601.

(45) B. Bozzini, A. Bund, B. Busson, C. Humbert, A. Ispas, C. Mele, and A. Tadjeddine, *Electrochem. Commun.*, 2010, **12**, 56–60.

(46) J. P. Zheng, P. C. Goonetilleke, C. M. Pettit, and D. Roy, *Talanta*, 2010, **81**, 1045–1055.

(47) L. Siinor, K. Lust, and E. Lust, *J. Electrochem. Soc.*, 2010, **157**, F83–F87.

(48) T. F. Esterle, D. Sun, M. R. Roberts, P. N. Bartlett, and J. R. Owen, *Phys. Chem. Chem. Phys.*, 2012, **14**, 3872–3881.

(49) Q. Zhang, Y. Han, Y. Wang, S. Ye, and T. Yan, *Electrochem. Commun.*, 2014, **38**, 44–46.

(50) A. J. Lucio, S. K. Shaw, J. Zhang, and A. M. Bond, *J. Phys. Chem. C*, 2017, **121**, 12136–12147.

(51) F. Silva, C. Gomes, M. Figueiredo, R. Costa, A. Martins, and C. M. Pereira, *J. Electroanal. Chem.*, 2008, **622**, 153–160.

(52) R. Costa, C. M. Pereira, and F. Silva, *Phys. Chem. Chem. Phys.*, 2010, **12**, 11125–11132.

(53) M. Ammam, D. Di Caprio, and L. Gaillon, *Electrochim. Acta*, 2012, **61**, 207–215.

(54) R. Costa, C. M. Pereira, and F. Silva, *RSC Adv.*, 2013, **3**, 11697–11706.

(55) A. Lewandowski, T. Majkowski, and M. Galiński, *Z. Naturfors.*, 2009, **64a**, 263–268.

(56) D. C. Grahame, *Chem. Rev.*, 1947, **41**, 441–501.

(57) B. B. Damaskin and O. A. Petrii, *J. Solid State Electrochem.*, 2011, **15**, 1317–1334.

(58) N. Nishi, J. Uchiyashiki, R. Oogami, and T. Sakka, *Thin Solid Films*, 2014, **571**, 735–738.

(59) N. Polyanovskaya and A. Frumkin, *Soviet Electrochem.*, 1970, **6**, 235–237.

(60) N. Grigorev, F. SA, and I. Bagotskaya, *Soviet Electrochem.*, 1972, **8**, 1590–1592.

(61) L. Doubova, V. Boitsov, and I. Bagotskaya, *Soviet Electrochem.*, 1978, **14**, 492–494.

(62) T. van Venrooij, M. Sluyters-Rehbach, and J. Sluyters, *J. Electroanal. Chem.*, 1999, **462**, 111–126.

(63) V. Emets, V. Mishuk, B. Damaskin, V. Elkin, and B. Grafov, *Russ. J. Electrochem.*, 2001, **37**, 1108–1114.

(64) L. M. Doubova, *Russ. J. Electrochem.*, 2010, **46**, 1230–1244.

(65) V. V. Emets and B. B. Damaskin, *Russ. J. Electrochem.*, 2015, **51**, 1149–1156.

(66) M. Carpenter and M. Verbrugge, *J. Electrochem. Soc.*, 1990, **137**, 123–129.

(67) P. Chen, Y. Lin, and I. Sun, *J. Electrochem. Soc.*, 1999, **146**, 3290–3294.

(68) L. H. S. Gasparotto, N. Borisenko, O. Hoefft, R. Al-Salman, W. Maus-Friedrichs, N. Bocchi, S. Z. El Abedin, and F. Endres, *Electrochim. Acta*, 2009, **55**, 218–226.

(69) G.-B. Pan, O. Mann, and W. Freyland, *J. Phys. Chem. C*, 2011, **115**, 7656–7659.

(70) J. Zhang, M. An, Q. Chen, A. Liu, X. Jiang, S. Ji, Y. Lian, and X. Wen, *Electrochim. Acta*, 2016, **190**, 1066–1077.

(71) M. Carpenter and M. Verbrugge, *J. Mater. Res.*, 1994, **9**, 2584–2591.

(72) Y. Traore, S. Legeai, S. Diliberto, G. Arrachart, S. Pellet-Rostaing, and M. Draye, *Electrochim. Acta*, 2011, **58**, 532–540.

(73) J. Estager, P. Nockemann, K. R. Seddon, G. Srinivasan, and M. Swadzba-Kwasny, *ChemSusChem*, 2012, **5**, 117–124.

(74) Y.-T. Hsieh, Y.-C. Chen, and I.-W. Sun, *ChemElectroChem*, 2016, **3**, 638–643.

(75) Y.-C. Liu, Y.-C. Chen, Y.-T. Hsieh, and I.-W. Sun, *J. Phys. Chem. C*, 2017, **121**, 8907–8913.

(76) M. J. Earle, C. M. Gordon, N. V. Plechkova, K. R. Seddon, and T. Welton, *Anal. Chem.*, 2007, **79**, 758–764.

(77) Q. Xu, N. Oudalov, Q. Guo, H. M. Jaeger, and E. Brown, *Phys. Fluids*, 2012, **24**, 063101(1–13).

(78) Y. Chung and C.-W. Lee, *J. Electrochem. Sci. Technol.*, 2013, **4**, 1–18.

(79) R. C. Chiechi, E. A. Weiss, M. D. Dickey, and G. M. Whitesides, *Angew. Chem.-Int. Edit.*, 2008, **47**, 142–144.

(80) V. B. Lazarev and Y. I. Malov, *Phys. Met. Metallogr.*, 1967, **24**, 186–188.

(81) S. Trasatti, *J. Electroanal. Chem.*, 1971, **33**, 351–378.

(82) J. J. Jasper, *J. Phys. Chem. Ref. Data*, 1972, **1**, 841–1009.

(83) V. Ivaništšev and M. V. Fedorov, *Interface*, 2014, **23**, 65–69.

Figure captions

Fig. 1 (a,b) Linear sweep voltammograms at 0.1 V s^{-1} and (c) electrocapillarity at the $[C_2mim^+]BF_4^-$|EGaIn (red line, red squares) interface, the $[C_8mim^+][C_4C_4N^-]$|EGaIn (blue line, blue diamonds) interface and the $[C_2mim^+]BF_4^-$|Hg (black open circles) interface[39] measured by the pendant drop method with error bars of one standard deviation. Vertical dotted lines are (a,b) at the potential where surface film is formed and (c) at the potential of zero charge at the $[C_2mim^+]BF_4^-$|Hg interface.

Fig. 2 Static differential capacitances as a function of the electrode potential (a) at the EGaIn (red squares) and Hg (black open circles)[39] interface of $[C_2mim^+]BF_4^-$ and (b) at the $[C_8mim^+][C_4C_4N^-]$|EGaIn (blue diamonds) and $[C_8mim^+]BF_4^-$|Hg (black open squares)[39] interface with error bars of one standard deviation. Dashed lines are fitted curves[39] using the EDL model[8,9] of ILs. Vertical dotted lines are at the potential of zero charge at the Hg interfaces.

Fig. A1 Differential capacitances as a function of the electrode potential (a) at the $[C_2mim^+]BF_4^-$|EGaIn interface and (b) at the $[C_8mim^+][C_4C_4N^-]$|EGaIn. Red squares and blue diamonds are the measured static differential capacitance, C_{dc} (same as those in Fig.2), black circles are the measured ac differential capacitance, C_{ac}. Red open squares and blue open diamonds are the static differential capacitance for the EDL of the ILs, $C_{dc,EDL}$.

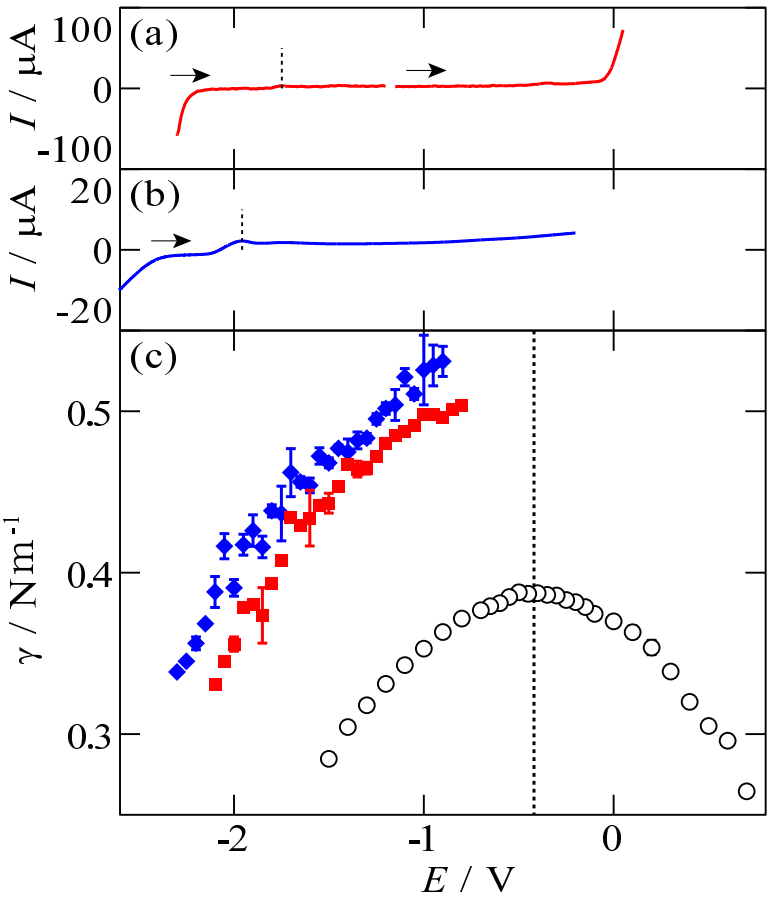

Fig.1 (Nishi et al.)

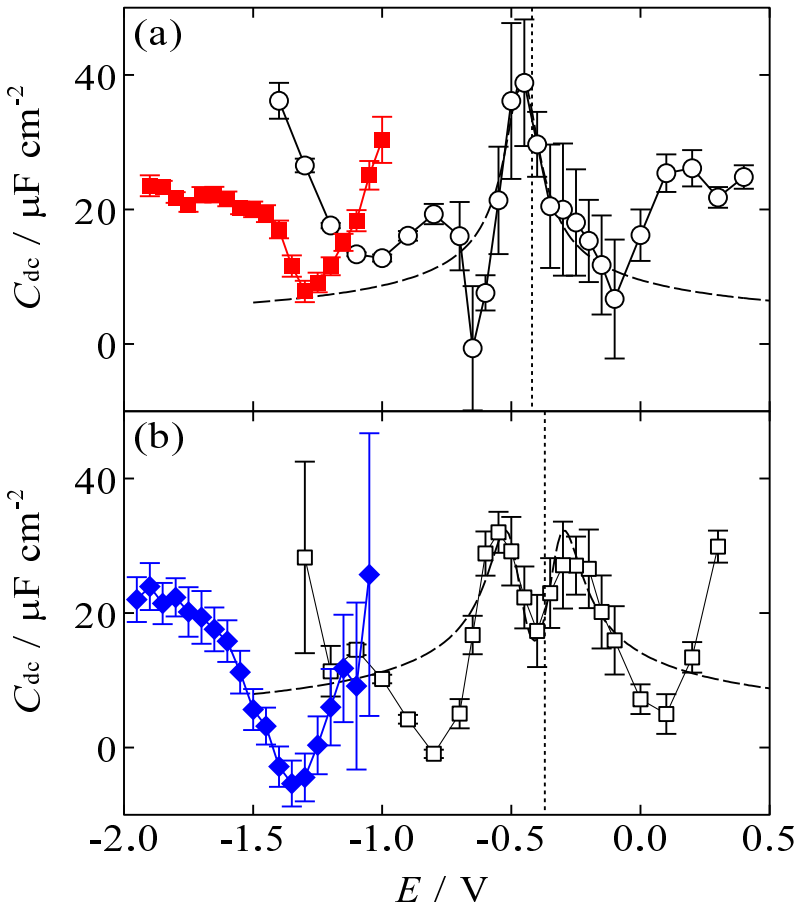

Fig.2 (Nishi et al.)

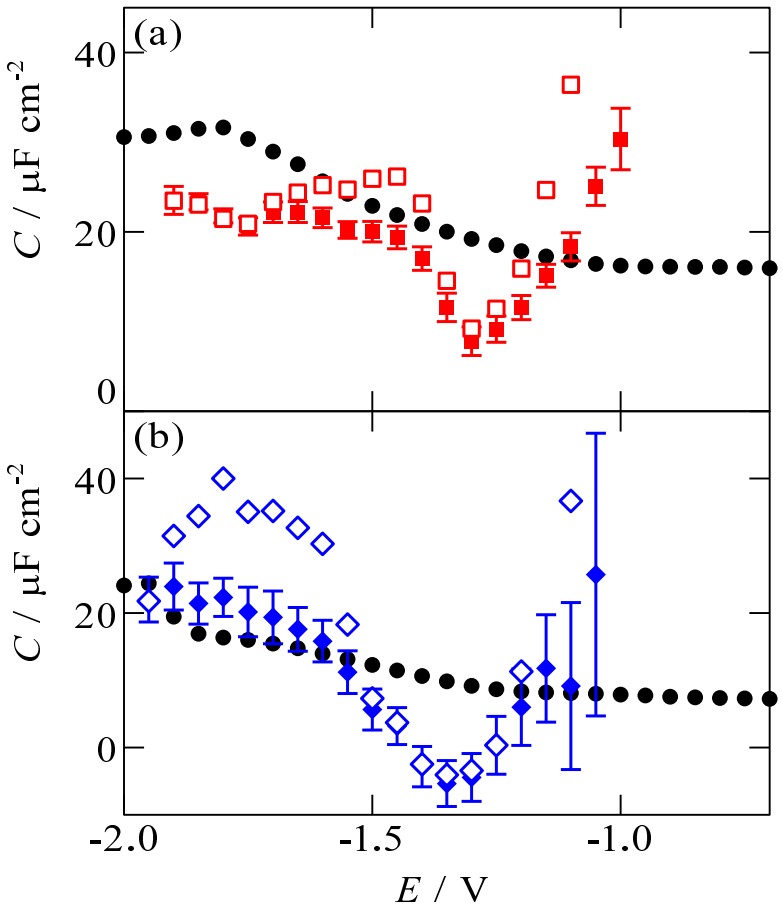

Fig.A1 (Nishi et al.)